

Article

Next-Generation IoT: Harnessing AI for Enhanced Localization and Energy Harvesting in Backscatter Communications

Rory Nesbitt¹, Syed Tariq Shah^{2,*} , Mahmoud Wagih¹ , Muhammad A. Imran¹ , Qammer H. Abbasi¹ 
and Shuja Ansari^{1,*} 

¹ James Watt School of Engineering, University of Glasgow, Glasgow G12 8QQ, UK; mahmoud.wagih@glasgow.ac.uk (M.W.); muhammad.imran@glasgow.ac.uk (M.A.I.); qammer.abbasi@glasgow.ac.uk (Q.H.A.)

² School of Computer Science & Electronic Engineering, University of Essex, Colchester CO4 3SQ, UK

* Correspondence: syedtariq.shah@glasgow.ac.uk or syed.shah@essex.ac.uk (S.T.S.); shuja.ansari@glasgow.ac.uk (S.A.)

Abstract: Ongoing backscatter communications and localisation research have been able to obtain incredibly accurate results in controlled environments. The main issue with these systems is faced in complex RF environments. This paper investigates concurrent localization and ambient radio frequency (RF) energy harvesting using backscatter communication systems for Internet of Things networks. Dynamic real-world environments introduce complexity from multipath reflection and shadowing, as well as interference from movements. A machine learning framework leveraging K-Nearest Neighbors and Random Forest classifiers creates robustness against such variability. Historically, received signal measurements construct a location fingerprint database resilient to perturbations. The Random Forest model demonstrates precise localization across customized benches with programmable shuffling of chairs outfitted with RF identification tags. Average precision accuracy exceeds 99% despite deliberate placement modifications, inducing signal fluctuations emulating mobility and clutter. Significantly, directional antennas can harvest over -3 dBm, while even omnidirectional antennas provide -10 dBm—both suitable for perpetually replenishing low-energy electronics. Consequently, the intelligent backscatter platform localizes unmodified objects to customizable precision while promoting self-sustainability.

Keywords: RFID; backscatter; RF energy harvesting; 6G; IoT; machine learning; localisation



Citation: Nesbitt, R.; Shah, S.T.; Wagih, M.; Imran, M.A.; Abbasi, Q.H.; Ansari, S. Next-Generation IoT: Harnessing AI for Enhanced Localization and Energy Harvesting in Backscatter Communications.

Electronics **2023**, *12*, 5020. <https://doi.org/10.3390/electronics12245020>

Academic Editors: Shibo He, Huan Zhou, Victor C. M. Leung, Fangyuan Xing and Lei Yang

Received: 16 October 2023

Revised: 5 December 2023

Accepted: 12 December 2023

Published: 15 December 2023



Copyright: © 2023 by the authors. Licensee MDPI, Basel, Switzerland. This article is an open access article distributed under the terms and conditions of the Creative Commons Attribution (CC BY) license (<https://creativecommons.org/licenses/by/4.0/>).

1. Introduction

Backscatter technology has been a promising area of research in recent years, with applications in various fields, such as low-power wireless communication [1,2], medical imaging [3,4], and secure authentication systems [5], which are always being hardened against attacks [6,7]. It is also commonly used in Internet of Things (IoT) systems, such as environmental monitoring [8] and battery-free IoT solutions [9–11]. In addition to its role in data transmission, backscatter communication (BSC) can also play a key role in the localisation of devices in 6G networks and effective densification of IoT devices [12,13]. Localisation is the act of determining an object's exact position within a set space; this can provide a range of benefits to 6G networks, including allowing wireless networks to dynamically adjust their settings based on the position of connected devices or improved location-based services, such as indoor navigation and augmented reality. Various localisation methods have been proposed over the years, using several measurement methods, such as radio frequency, inertial measurements, visible light, ultrasound, and different hybrid applications. Since cellular and wireless local area network (WLAN) infrastructures are prevalent in modern wireless communication systems and bring value to user-oriented services and network management, RF signals are among these modalities that are most frequently used [12], and they will be the focus of our research.

Localisation in 6G is an active research area within IoT, and the concept of backscatter localisation has been explored in the recent literature. In [14], the authors designed a radio simultaneous localisation and mapping (R-SLAM) algorithm using Terahertz (THz) frequencies, which is less computationally heavy than state-of-the-art R-SLAM techniques, and provide an evaluation of backscattering using the THz channel. They found that simplified Fourier–Mellin (SFM) gave the best trajectory estimation for an object out of the algorithms they tested as it was less affected by image artefacts. They concluded that using personal radar is feasible to create infrastructure-less localisation and mapping in future 6G systems.

The authors in [15] propose a wireless localisation system that uses re-configurable intelligent surfaces (RISs). The RISs are smart metasurfaces that can change the direction which reflect radio signals; therefore, they can direct the wireless signals more directly toward the reader. In [15], they propose machine learning and heuristic algorithms to select a smaller subset of RIS configurations for near-optimal localisation accuracy. Through the use of simulations, they conclude that such an algorithm will provide a 33% accuracy increase compared to a random selection of RIS configurations while still being able to scale to multiple simultaneous users. A method of using visible light backscatter (VLB) for localisation is looked at in [16]. VLB tags work similarly to BSC tags, modulating the visible light (rather than radio waves) from a light-emitting diode (LED) using an LCD shutter or advanced metasurfaces to control reflection. Lastly, the receiver antenna is replaced by photodiodes, which can detect the light shining on them. The authors propose using VLB systems in healthcare to avoid repeat exposure to more traditional backscatter radio waves.

The lack of a battery requirement for BSC technology has led authors in [17] to look at using it for in-body localisation. Since backscatter requires zero transition power and therefore does not need a battery, they propose its use to decrease the size of micro-implants which are put inside a person's body, known as deep-tissue backscatter. This idea brings many challenges due to the nature of human skin, which they overcame using a ReMix backscatter system. Using chicken meat and human phantom tissue, they found that localisation was possible to an accuracy of at least 2.2 cm. A fingerprinting method using 6G communication is explored in [18] for vehicle-to-infrastructure communication, which is used to localise an antenna attached to a vehicle, comparing position-assisted and radar-assisted beam management (BM) with a multi-technology BM solution. They find that the best BM performance comes when the vehicle-to-base-station communication is constant. However, this is unlikely to happen in a real-world situation, and therefore the authors conclude that both positionally assisted and radar-assisted BM solutions are required for a working system and the accurate localisation of a vehicle's radar remains an open problem.

In [19], passive RFID tags are analysed for use in a library localisation system for books. The research proposes passive ultra-high frequency (UHF) RFID tags for use in their book-localisation system. The authors use a simulation to show how this system can capture a book's true position in the library. One main reason they propose a new library system is the high probability of current systems misreading books; that is to say, the systems would misidentify a book's ID number. The system they simulate assumes that the Received Signal Strength correlates with the distance and that the library will remain static. With these assumptions, they state that their system can significantly increase performance and accuracy without needing extra resources compared to current methods.

This paper aims to explore the possibilities of utilising BSC in developing next-generation 6G mobile networks; 6G, the successor of the current wireless technology, promises to offer exceptional speed and dependability in connectivity. Among the various communication techniques, BSC stands out for its ability to facilitate communications with minimal power and resources, making it a promising contender in fulfilling the goals of 6G in providing massive connectivity to end devices with optimum energy efficiency. A backscatter tag modulates data onto an RF signal while simultaneously reflecting the signal, as explained in Section 2. After modulation, the signal has been modified to carry new data, which are then decoded when they return to the reader. As backscatter relies on

reflecting or scattering existing signals rather than transmitting its own, it offers a potential solution to the battery-related challenges faced by Internet of Things (IoT) applications. In comparison to traditional communication methods, BSC requires much less energy, making it an attractive option for IoT devices that need to operate for an extended period without charging.

Building upon and addressing the shortcomings in previous studies, this paper investigates the advantages and obstacles of implementing BSC in upcoming wireless IoT networks, as well as its role in developing a more energy-efficient and sustainable localization technique. The technical aspects of BSC are scrutinized, focusing on its integration into 6G networks and its potential influence on the overall performance of these networks. Through a comprehensive analysis of BSC's function in 6G and its prospects for sustainability, this research seeks to offer valuable insights into the future landscape of the 6G-enabled Internet of Things (IoT).

This goal is accomplished by introducing a machine learning (ML) model that precisely forecasts the placement of Radio Frequency Identification (RFID) tags within a predetermined area. The demonstration involves a testbed featuring eight tagged targets (chairs, in this case) surrounding a large desk. The testbed supports consistent experimentation in an indoor setting resembling a workplace. The study emphasizes the crucial parameters that enhance the model's accuracy and examines the effects of changing these parameters. Moreover, the research delves into the prospects of utilizing these technologies to establish a low-energy IoT network, capitalizing on their innate energy efficiency.

The following are the main contributions of this paper:

1. A comprehensive overview of the current state of localisation with backscatter and its significance in future 6G networks.
2. Implementing a testbed that allows the evaluation of RFID-based BSC technologies in a complex indoor environment. The RF signal strength at different positions within the testbed and its effect on the result is also examined.
3. Development and evaluation of the RFID-based machine learning model for indoor localisation and occupancy monitoring
4. Experimental demonstration of indoor localisation along with a detailed RF power survey, evidencing the possibility of having localisation and energy harvesting in the same space, including a discussion on the effect of varying parameters.
5. An outlook on applying similar methods in the future to create energy-efficient IoT networks, leveraging the unique benefits of BSC technology.

The structure of this paper is organized as follows. Section 2 analyzes the strengths and limitations of BSC technology and its potential impact on 6G networks. Section 3 presents the system model, including the arrangement of BSC tags for optimal performance and the positioning of the RF antenna. The implementation of the proposed approach is examined in Section 5, offering a detailed overview of the techniques and methods utilized. Section 6 discusses the performance of the approach and the effects of varying parameters. Section 4 explores the potential of harnessing energy lost during localization. Finally, Section 7 concludes the findings and suggests potential applications for the work.

2. The State of the Art in Backscatter Communication

Backscatter works by reflecting a signal of the device and reading the scattered data when that signal is received at the reading device. When scattering a signal, the BSC device will modulate it with a specified string of data [20], which the reader can understand. This data, combined with information about the transition, such as the Received Signal Strength Indicator (RSSI) of the returned signal, allows for a huge range of intelligent use cases. Most modern debit cards use a form of BSC called NFC [21], allowing contactless payments.

The process of modulating data works by changing the load impedance, affecting the amplitude or phase of the reflected signal [22]. This is the main advantage seen in such set-ups as the device uses the power already in the transmitted signal (which is very low) to modulate the data onto it. This means that passive BSC devices require no external

power source, such as a battery, and the system can expand with more BSC devices without increasing the total power usage at all, provided the reader can handle that many devices. Another benefit is cost, as individual BSC tags are very cheap to produce compared to battery-powered sensors.

Backscatter set-ups come in two main types: dedicated and ambient. Dedicated backscatter can be either monostatic, where both the transmission and reading are performed by the same device, or bistatic, where there can be one or multiple transmitters to send the unmodulated signal and a separate reader to receive the modulated signal. Ambient backscatter has no transmitter but rather uses the RF signals already in the environment; therefore, it does not need the same power infrastructure as a dedicated backscatter [2,23]. The result of ambient BSC is unmatched power efficiency per byte of data transferred, effectively transmitting data out of thin air. No matter which form of backscatter is used, the BSC device reflects back RF signals while changing its reflection coefficient to modulate the signal [20]. This process uses only the power in the RF signal, which is very low energy.

As 6G networks begin to take shape, backscatter communication is poised to play a critical role in strengthening the next generation of wireless communication. With its ability to transmit data using ambient RF signals, backscatter communication can support a wide range of low-power and low-cost devices, such as IoT sensors, that are expected to be a major component of 6G networks. Furthermore, backscatter communication can coexist with existing wireless technologies, making it an ideal solution for dense urban environments where spectrum availability is a major challenge. The 6G networks are expected to deliver ultra-high-speed, ultra-low-latency, and ultra-high-reliability communication. Backscatter communication can help support these requirements by providing a scalable and efficient communication method with numerous devices. It has been shown by [2] that a BSC device can be connected to the internet by backscattered Wi-Fi signals; this same idea can be applied to 6G BSC devices to allow for fast communication between devices and out to the internet. As a result, backscatter communication is expected to be an integral part of developing 6G networks.

3. Localisation for Backscatter Communications

By reflecting or modulating ambient RF signals, backscatter-enabled devices can transmit information about their location, or it can be calculated from the received data, which can be used to determine their precise position. Furthermore, the high-speed and low-latency communication capabilities of 6G networks can support the real-time localisation of devices with high precision. The combination of backscatter communication and 6G networks can thus enable new use cases and services that were not possible with previous generations of wireless technology. Backscatter can be used in many ways for localisation. One proposed method is to triangulate the signal with multiple RF readers [24], and another method uses the RSSI of the signal when it is received at the reader to determine the distance, from which it is possible to calculate its exact location [25]. In this paper, the comparison of RSSI and phase-angle values is made against a known fingerprint of the location to determine the position of each tag.

System Model: Testbed Environment

In this paper, the concept of backscatter localization, combined with machine learning algorithms, was employed for tracking the position of chairs. More specifically, this study concentrated on evaluating the Received Signal Strength Indicator (RSSI) and phase angle in a controlled, work-like environment. A testbed was constructed, featuring eight chairs arranged around a desk. Figure 1 depicts these chairs around the desk, each positioned corresponding to its number (for example, chair 1 is at position 1). The setup included two ultra-high-frequency (UHF) antennas, with one situated at the desk's centre and the other placed to one side. The desk was located in a low-traffic but actively used area and outfitted with multiple monitors. This location choice facilitated the evaluation of

the machine learning model in conditions that closely resemble those of a high-traffic real-world environment.

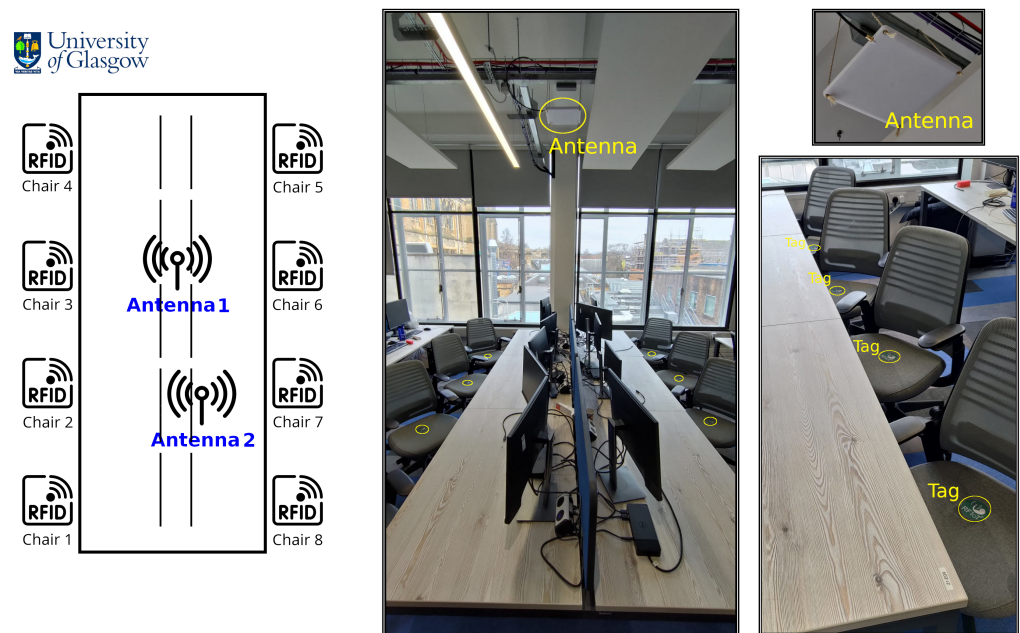


Figure 1. Layout of the RFID tags and antenna around the testbed desk.

The values obtained from the testbed exhibited a degree of fluctuation; however, a discernible pattern allowed us to train the ML algorithms, as discussed in Section 5.2. Each chair was equipped with a single RFID tag on the base of the chair, as shown in Figure 1. These tags all have a constant identifier followed by the chair number set as their EPC value so they can be tracked appropriately when looking back on the readings. The chair number was directly tied to its position around the desk, as depicted in Figure 1. Initially, the idea of using multiple tags per chair was explored, but this approach negatively affected the data collection process. It was observed that each tag could display a significantly different RSSI or phase angle, even when being read simultaneously. The antennas were suspended above the desks as shown in Figure 1.

4. Energy Harvesting Potential in an RFID Sensing Network

4.1. RF Energy Harvesting Literature

Ambient RF energy harvesting has been demonstrated in several applications using not just RFID signals [11,26] but also including WiFi [27,28], radio [29,30], digital television [31,32], underwater communication [33], and of course, solar energy [34] (Ref. [32], Shunde, China [35]). Additionally, similar surveys have taken place for indoor office environments [36,37].

In [38], a comprehensive analysis of RF energy harvesting is carried out to address the gap in understanding the factors influencing performance. The study delves into the available power density, emphasising RF energy harvesting potentials, the factors affecting its performance, and its diverse applications. It also explores various research aspects essential for RF energy harvesting, encompassing harvesting sources, evaluation metrics, energy propagation models, rectenna architectures, and MAC protocols. Furthermore, the authors recommend future research directions, specifically enhancing DC output power and rectenna sensitivity.

It was found that single ambient frequency levels are not sufficient for this purpose as they can be below -40 dBm [31,32,39] and sometimes even below -60 dBm at frequency ranges of 550 MHz to 2.5 GHz [35,36]. However, using multi-band power, the authors in [40] were able to measure a level of -15 dBm. Even with multi-band power, these levels

remain at levels less than we could harvest from our RFID testbed, discussed in more detail in Section 4.2.

Another approach that has been seen in the literature is to make use of mobile transmitters to provide the ambient RF power, either from mobile phones [41] or license-free sources [42,43]. Studies in this area have reached power levels of 1.88 dBm [41] by keeping the distance between the transmitter and the RF harvesters very low (18 cm). In [42], the authors used 3D EM field simulations to estimate the electric and magnetic (E and H) near-field power received on a wearable wristband receiver transmitted from a two-way radio. They confirmed their simulations with E- and H-probes on their wrist, from which they designed an antenna intended to be mounted on a person's wrist.

The authors in [44] explore RF energy harvesting for IoT sensors using a slotted bow-tie antenna. They aim to exploit multiple frequency bands to efficiently convert ambient RF signals into usable DC power, removing the need for traditional power sources. Using a dual-band receiver allows the energy harvester to collect more power [34]. The authors in [34] were able to power a device from a 6.3 km distance using UHF digital TV signals.

4.2. Energy Level Analysis

Using a spectrum analyser, we were able to measure the RF energy received by a simple omnidirectional dipole antenna of approximately two dBi gain and a uni-directional version of the antenna. The uni-directional antenna was implemented by backing the dipole antenna with a reflector, creating broadside radiation patterns, which increases the gain by approximately 3 dB [45] when compared to a free-standing omnidirectional antenna.

Shown in Figure 2a,b is a heat map of the whole room area, where zones 3 and 4 combine to be the test location for our localisation experiment. Figure 2a shows the energy levels using an omnidirectional antenna, and Figure 2b shows the unidirectional UHF antenna. All readings were taken on the desks or the arm of a chair for positions between desks. The antennas were positioned 218 cm above the desk (one antenna was set at a height of 208 cm due to the room structure, which would have blocked it at the full height), and the chairs were positioned a further 20 cm down.

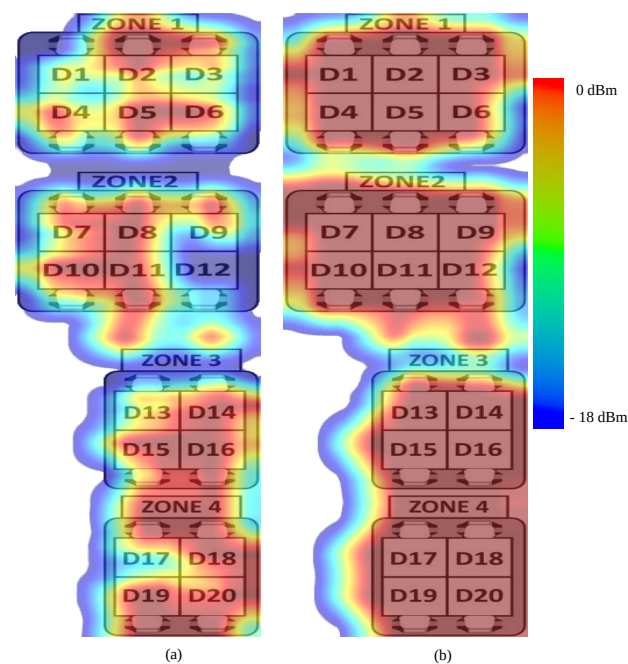


Figure 2. Heat map of the received RF power with (a) omnidirectional and (b) uni-directional antennas.

This observation reveals hot spots near the antenna, particularly in Figure 2 around position D5, though the entire area exhibits some degree of RF radiation. The available energy was observed to diminish with increasing distance from the antenna until nearing a

wall, where an increase in energy level was noticed. This variation in signal strength could account for certain inaccuracies in localisation since the signal reaching the tag directly and the one reflecting off the wall will possess distinct values. These variations are known as the multipath components of the transmitted signal.

In Figure 3, we can see that with the omnidirectional antenna, half of the room is at or above -10 dBm, which is still very low but could be collected over time. Half of the room is above -3 dBm for the uni-directional antenna, which is a much more usable power level. It's clear from this that the energy required to power a device constantly is not available throughout the room but is possible in some high-powered regions. However, the energy is enough to be collected over time to power a device for short bursts without needing a battery. It also clarifies that using a directional antenna over an omnidirectional one has a huge benefit.

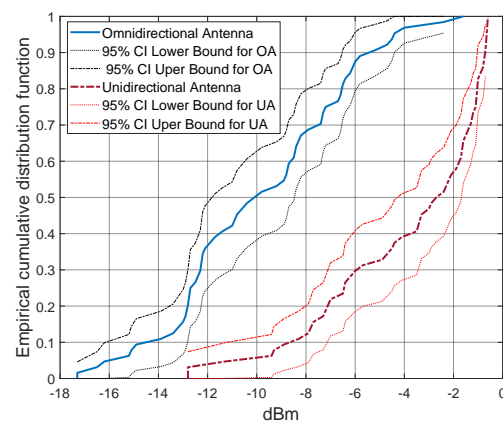


Figure 3. Comparative CDF of the received power from the RFID signal for each antenna.

These transmitters radiate over 30 dBm of equivalent isotropic radiated power (EIRP). In our testing, we were able to harvest this at a consistent 1 V or higher at up to an 85 cm distance, using the same antenna on a Powercast P210-EVB Powerharvester. Figure 4 shows the sustainable DC voltage that was able to be harvested compared with the distance between the transmitting antenna and the harvester receiving antenna; 4.2 V is the maximum that the Powercast board can output.

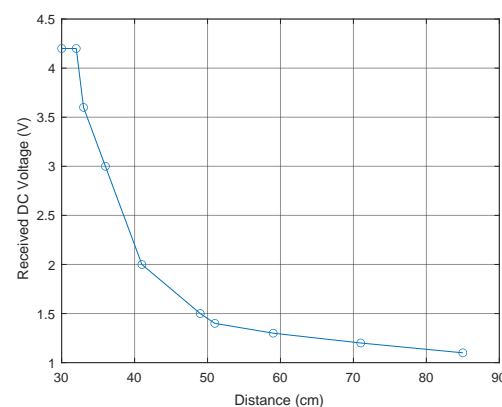


Figure 4. Power harvested from the RFID signal at different distances from the RF reader.

Adding an energy harvester should have a negligible effect on the existing system power requirements. One possible route to further this research is to use such readings to train an ML system to build a map of the room energy level. This system could then be used to predict the efficiency of energy harvesting devices at different locations in the room.

5. AI-Enabled Localisation Experimentation

This section outlines the methodology employed for identifying the desk location using radio frequency (RF) signals. The system was developed by utilizing RSSI and phase-angle parameters along with two algorithms: K-Nearest Neighbours (KNN) and Random Forest. The testbed setup was utilized to create a fingerprint of the area during data collection, followed by testing readings with chairs in both their original and mixed-up positions.

Our process for training is as shown in Algorithm 1.

Algorithm 1: Supervised ML Training

Data: RSSI(n), $\theta(n)$ at home position
Result: predicted location of all chairs
for Chair n in each location l **do**
 | Store RSSI(n) and $\theta(n)$ for position l
end
for Each Model m **do**
 | TrainData \leftarrow 80% stored data randomly
 | TestData \leftarrow 20% left over stored data
 | Train m on TrainData
 | Test m on TestData
end
Select a model for live testing
while live data is available **do**
 | $d \leftarrow$ data collected over 5 seconds
 for each chair n in d **do**
 | RSSI \leftarrow average RSSI for $d(n)$
 | $\theta \leftarrow$ average θ for $d(n)$
 | location(n) \leftarrow prediction from RSSI and θ
 end
end

5.1. Data Collection

The process began by creating a fingerprint of the area. Each chair was placed in its designated position, followed by data collection for the system. This fingerprint included five-second average values for both the RSSI value and phase angle, gathered over a twenty-minute period. The chair number and position were also recorded during the test. Subsequently, this procedure was replicated with the chair positioned directly under the desk, where there would be no line of sight to the antenna. It was then repeated with the chair pulled out 20 cm from the desk, ensuring a direct line of sight with the reader. The data collection was conducted in an environment free of humans or obstacles.

5.2. Algorithm Implementation

The machine learning models estimate the chair's location from the input of RSSI and phase angle; the predicted output was an integer representing the desk location. RSSI was stable, although it could jump slightly. The phase angle had a wider range of values but could also jump unexpectedly at certain points. The RSSI can be calculated as follows:

$$\text{RSSI} = -10n \log_{10}(d) + A, \quad (1)$$

where d is the distance between the transmitter and receiver, n is the path loss exponent, and A is the RSSI offset. This equation relates the RSSI to the distance between the transmitter and receiver, where the RSSI decreases as the distance increases due to signal attenuation. The path loss exponent n and the RSSI offset A are parameters that can be calibrated based on the specific wireless environment and hardware used.

In other words, the larger the distance between the antenna and the RFID tag is, the lower the RSSI value is when the signal returns to the antenna. For localisation, this relationship between RSSI and physical distance can be utilised. To do so, we compare the latest RSSI value with the stored fingerprint value, allowing us to know the distance between the reader and each marked position by saving the RSSI at each location.

The calculation for phase angle changes depends on many factors, such as monostatic vs. bistatic configurations. The RF reader calculates this value by contrasting the phase of the local oscillator, which creates the wave that will be modulated by the tag, with the phase of the field backscattered by the tag. Equation (2), which applies to bistatic configurations, comes from [46].

$$\Phi(\vec{r}) = \left(\frac{2\pi}{\lambda} R_D + \varphi_{Tx-Rx} \right) - \left(\frac{2\pi}{\lambda} [R_T(\vec{r}) + R_R(\vec{r})] + \varphi_{Tx-tag}(\vec{r}) + \varphi_{tag-Rx}(\vec{r}) \right) + \phi_0 \quad (2)$$

where R_D is the direct path transmitter–receiver, R_T is the tag, R_R is the receiver, \vec{r} is the tag position, and λ is the wavelength of the signal.

We tested two algorithms, KNN and Random Forest, to determine the desk location.

KNN is a simple yet effective machine-learning algorithm for classification and regression tasks. Given a new input vector, KNN finds the K-closest training examples in the feature space and predicts the output label as the mode of the K-nearest class labels. The predicted value for regression is the average of the K-nearest output values. To find the distance, KNN uses Euclidean distance, which can be expressed as [47]

$$d(A, B) = \sqrt{(x_1 - x_2)^2 + (y_1 - y_2)^2}, \quad (3)$$

KNN does not make any assumptions about the underlying data distribution. However, it can be computationally expensive for large datasets.

Alternatively, Random Forest, as defined in [48], is a popular machine-learning algorithm that uses an ensemble of decision trees to make predictions. The algorithm randomly selects a subset of features for each tree and partitions the data recursively based on the selected features. The predicted output label is the mode of the class labels predicted by the individual trees or the average in the regression case. Random Forest is a powerful and versatile algorithm that can handle large datasets with many features and capture linear and non-linear relationships between the input features and the output labels. Random Forest is a powerful ensemble method and works better with large datasets with many features. At the same time, KNN is more straightforward and interpretable but does not scale as well as Random Forest. Although we tested with both, we focused mainly on Random Forest as the performance advantage made working with live data and getting up-to-date results much more feasible.

5.3. Results

5.4. Data Analysis

The results showed that the 5 s average readings provided the most desirable outcomes for the use case. We found that using only 3 s averages would not be enough to account for inconsistencies, with no significant difference between 5 s and 10 s average readings. However, the two antennas in certain zones did not detect some desks. The addition of a third antenna significantly improved the accuracy of the system. As seen in Figure 5a, while accuracy is very high, there were several incorrect predictions during our testing. Figure 5b shows that the additional antenna completely removed the wrong predictions.

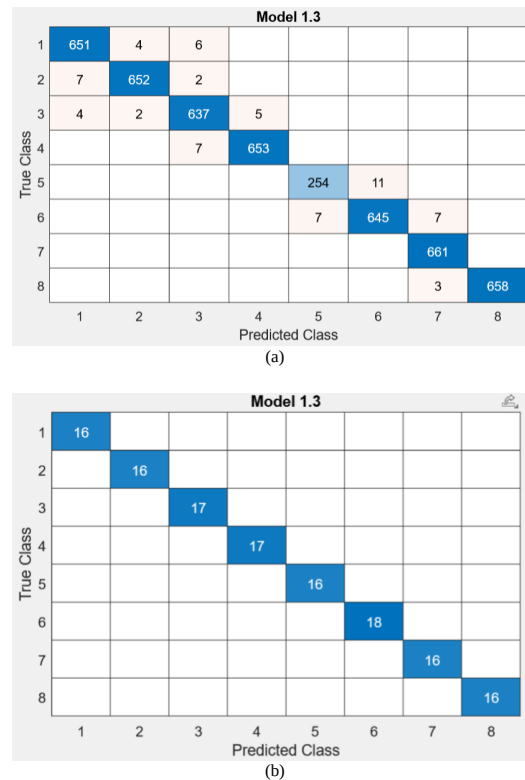


Figure 5. Confusion matrix of the RFID-based localisation using two reader antennas (a) vs. three reader antennas (b).

The test data showed that the system could accurately determine the location of the desks in a work-like environment. The results were affected by the presence of people at the desks or walking around the room. Despite the sometimes erratic nature of the phase angle, its inclusion in the model improved the system's overall accuracy.

6. Evaluation of Performance

To evaluate the model, we set up a system to take readings over 5 s, average the values, and then run this through the model for each chair. This was performed in a live environment with equipment such as laptops/monitors on the desks, more so than during training, as well as people around the room and sometimes at the desk area. If the antenna cannot pick up a tag, it is assumed that the chair is occupied and not included in the output. Each set of readings given to the model was fed blindly, so there was no chance of the correct result being wrongly factored into the testing. Only after receiving a prediction was this checked for accuracy.

When using only 2 antennas, we yielded a result of 82% correct predictions while using the Random Forest algorithm, which we were able to improve up to 93% correct when adding in the third antenna. When comparing these results, it is clear that additional antennas make a notable difference; however, this solution is not feasible for most applications due to the monetary cost involved. We instead focused on improving accuracy with fewer antennas.

Figure 6 shows specific results from a small selection of tests while Figure 7 shows the high levels of accuracy we were able to reach when focusing on honing Random Forest with two antennas. From this, we can see the accuracy reaches 100% while the chairs are all in their original position; however, predictions remain precise while chairs are moved, and most mistakes are only out by one.



Figure 6. Number of correct predictions for different models.

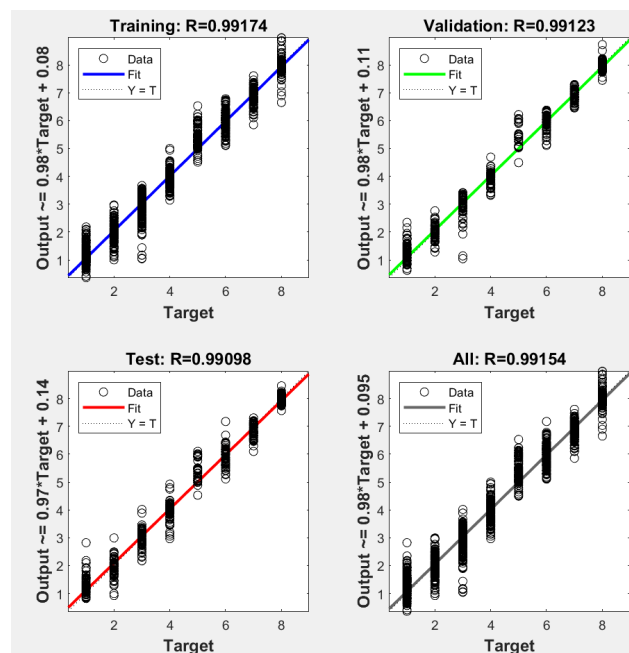


Figure 7. Validation for Random Forest; R is accuracy.

Figure 7 displays regression plots used for statistical analysis to examine the relationship between the output and target variable. The data points show the actual observations, while the fitting line represents the predicted values. The R score is the correlation coefficient, which indicates the relation between the predicted and target values. On the Y-axis of each plot, you can find an equation (e.g., $Output = 0.987 \times Target + 0.08$) that represents the linear regression equation fitted to the data, where the coefficient (0.987) is the slope and the constant term (e.g., 0.08) is the intercept. This equation is derived from model training, and the correlation coefficient R is a statistical measure that determines the strength and direction of a linear relationship between two variables. The R scores of training, validation, and test are almost identical and close to 1, indicating that the model does not suffer from overfitting.

7. Conclusions and Future Work

In this paper, we have analysed the current state of backscatter communication and its potential in future 6G networks, and we have looked at the state of the art of RF localisation. While many methods for localising objects using RFID tags exist, they have flaws. Our solution takes known positional readings to create a fingerprint of the area and then uses Random Forest ML to predict in real-time which of our known locations each

tag is currently in. Combining our fingerprint method and using defined locations over exact coordinates allows our algorithm to run in a real-world environment with objects and people coming and leaving. We Found Random Forest to be more advantageous than KNN due mainly to its speed benefits, as this allows the system to run more regularly on low-power hardware. We have shown that RF localisation can provide highly accurate results in a controlled environment and, with some preparation, can hold up to the chaos of working environments. Our system provided nearly 100% results, even when people or devices were present. However, while tuning the model to get to that 100%, we noticed that possible multipath issues were affecting results close to reflective objects. Furthermore, we found that such systems leave a lot of energy available in the room and propose using RF energy harvesting when such systems are in use. Through ML, it would be possible to predict the best locations in the environment to place energy harvesting devices that would optimise their power generation. Our future work focuses on developing a method for fully blind localization, enabling a system that operates without specific training for each new environment. This innovation could significantly enhance the adaptability and efficiency of IoT networks in various settings. Additionally, we aim to deepen our investigation into multipath issues, particularly the effects of environmental changes like the addition or removal of reflective surfaces. By incorporating a specialized pre-processing step in our machine-learning algorithm, we plan to detect and effectively counteract multipath components, thus improving system performance and reliability in diverse scenarios.

Author Contributions: Conceptualization, R.N., M.W. and S.A.; Methodology, R.N., S.T.S. and M.A.I.; Software, R.N.; Validation, R.N.; Formal analysis, S.A.; Investigation, S.T.S. and Q.H.A.; Data curation, M.W.; Writing—original draft, R.N.; Writing—review and editing, S.T.S., M.W., M.A.I., Q.H.A. and S.A.; Supervision, M.A.I., Q.H.A. and S.A. All authors have read and agreed to the published version of the manuscript.

Funding: This research received no external funding.

Data Availability Statement: Data is contained within the article.

Conflicts of Interest: The authors declare no conflict of interest.

References

1. Toro, U.S.; Wu, K.; Leung, V.C.M. Backscatter Wireless Communications and Sensing in Green Internet of Things. *IEEE Trans. Green Commun. Netw.* **2022**, *6*, 37–55. [CrossRef]
2. Kellogg, B.; Parks, A.; Gollakota, S.; Smith, J.R.; Wetherall, D. Wi-Fi Backscatter: Internet Connectivity for RF-powered Devices. In Proceedings of the 2014 ACM Conference on SIGCOMM, Chicago, IL, USA, 17–22 August 2014; pp. 607–618. [CrossRef]
3. Zhou, Z.; Gao, A.; Zhang, Q.; Wu, W.; Wu, S.; Tsui, P.H. Ultrasound Backscatter Envelope Statistics Parametric Imaging for Liver Fibrosis Characterization: A Review. *Ultrason. Imaging* **2020**, *42*, 92–109. [CrossRef] [PubMed]
4. Zhou, Z.; Zhang, Q.; Wu, W.; Wu, S.; Tsui, P.H. Hepatic Steatosis Assessment Using Quantitative Ultrasound Parametric Imaging Based on Backscatter Envelope Statistics. *Appl. Sci.* **2019**, *9*, 661. [CrossRef]
5. D’Arco, P.; De Santis, A. On Ultralightweight RFID Authentication Protocols. *IEEE Trans. Dependable Secur. Comput.* **2011**, *8*, 548–563. [CrossRef]
6. Wang, P.; Yan, Z.; Zeng, K. BCAuth: Physical Layer Enhanced Authentication and Attack Tracing for Backscatter Communications. *IEEE Trans. Inf. Forensics Secur.* **2022**, *17*, 2818–2834. Available online: <https://ieeexplore.ieee.org/abstract/document/9845476> (accessed on 20 August 2023). [CrossRef]
7. Mehmood, A.; Aman, W.; Rahman, M.M.U.; Imran, M.A.; Abbasi, Q.H. Preventing Identity Attacks in RFID Backscatter Communication Systems: A Physical-layer Approach. In Proceedings of the 2020 International Conference on UK-China Emerging Technologies (UCET), Glasgow, UK, 20–21 August 2020; pp. 1–5. [CrossRef]
8. Gupta, V.; Tripathi, S.; De, S. Green Sensing and Communication: A Step Towards Sustainable IoT Systems. *J. Indian Inst. Sci.* **2020**, *100*, 383–398. [CrossRef]
9. Shah, S.; Choi, K.; Hasan, S.; Chung, M. Energy harvesting and information processing in two-way multiplicative relay networks. *Electron. Lett.* **2016**, *52*, 751–753. [CrossRef]
10. Jameel, F.; Zeb, S.; Khan, W.U.; Hassan, S.A.; Chang, Z.; Liu, J. NOMA-Enabled Backscatter Communications: Toward Battery-Free IoT Networks. *IEEE Internet Things Mag.* **2020**, *3*, 95–101. [CrossRef]
11. Shah, S.T.; Choi, K.W.; Hasan, S.F.; Chung, M.Y. Throughput analysis of two-way relay networks with wireless energy harvesting capabilities. *Ad Hoc Netw.* **2016**, *53*, 123–131. [CrossRef]

12. Chen, H.; Sardeddeen, H.; Ballal, T.; Wymeersch, H.; Alouini, M.S.; Al-Naffouri, T.Y. A Tutorial on Terahertz-Band Localization for 6G Communication Systems. *IEEE Commun. Surv. Tutorials* **2022**, *24*, 1780–1815. [[CrossRef](#)]
13. Shah, S.T.; Choi, K.W.; Lee, T.J.; Chung, M.Y. Outage Probability and Throughput Analysis of SWIPT Enabled Cognitive Relay Network With Ambient Backscatter. *IEEE Internet Things J.* **2018**, *5*, 3198–3208. [[CrossRef](#)]
14. Lotti, M.; Pasolini, G.; Guerra, A.; Guidi, F.; D’Errico, R.; Dardari, D. Radio SLAM for 6G Systems at THz Frequencies: Design and Experimental Validation. *arXiv* **2022**, arXiv:2212.12388.
15. Nguyen, C.L.; Georgiou, O.; Gradoni, G.; Di Renzo, M. Wireless Fingerprinting Localization in Smart Environments Using Reconfigurable Intelligent Surfaces. *IEEE Access* **2021**, *9*, 135526–135541. [[CrossRef](#)]
16. Ullah, M.H.; Gelli, G.; Verde, F. Visible Light Backscattering with Applications to Communication and Localization in Healthcare: A Survey. *Procedia Comput. Sci.* **2022**, *203*, 745–752. [[CrossRef](#)]
17. Vasisht, D.; Zhang, G.; Abari, O.; Lu, H.M.; Flanz, J.; Katabi, D. In-Body Backscatter Communication and Localization. In Proceedings of the SIGCOMM ’18: 2018 Conference of the ACM Special Interest Group on Data Communication, New York, NY, USA, 20–25 August 2018; pp. 132–146. [[CrossRef](#)]
18. Linsalata, F.; Tagliaferri, D.; Rinaldi, L.; Bezzetto, L.; Mizmizi, M.; Scazzoli, D.; Badini, D.; Mazzucco, C.; Magarini, M.; Spagnolini, U. Localizing the Vehicle’s Antenna: An Open Problem in 6G Network Sensing. *arXiv* **2022**, arXiv:2204.01097.
19. Bi, S.; Wang, C.; Wu, B.; Gong, Y.; Ni, W. An Accurate Book-Localization Approach Based on Passive Ultra-High-Frequency RFID. In *Lecture Notes in Electrical Engineering, Proceedings of the 6th International Technical Conference on Advances in Computing, Control and Industrial Engineering (CCIE 2021)*; Shmaliy, Y.S., Abdelnaby Zekry, A., Eds.; Springer: Singapore, 2022; pp. 584–591. [[CrossRef](#)]
20. Bletsas, A.; Dimitriou, A.G.; Sahalos, J.N. Improving Backscatter Radio Tag Efficiency. *IEEE Trans. Microw. Theory Tech.* **2010**, *58*, 1502–1509. [[CrossRef](#)]
21. Pinho, P. *Recent Wireless Power Transfer Technologies*; BoD—Books on Demand: London, UK 2020.
22. Nagaraj, S. Spectrum Shaping for Backscatter Modulation. *ICT Express* **2017**, *3*, 52–55. [[CrossRef](#)]
23. Basharat, S.; Hassan, S.A.; Mahmood, A.; Ding, Z.; Gidlund, M. Reconfigurable Intelligent Surface-Assisted Backscatter Communication: A New Frontier for Enabling 6G IoT Networks. *arXiv* **2021**, arxiv:2107.07813.
24. Abdullah, A.N.; Abdul-Rahaim, L.A. Enhancing the Performance of Localization System for Radio Frequency Transmitters Based on DOA and Triangulation Algorithms. *Int. J. Eng. Trends Technol.* **2021**, *69*, 26–35. [[CrossRef](#)]
25. Zhao, Y.; Liu, K.; Ma, Y.; Gao, Z.; Zang, Y.; Teng, J. Similarity Analysis-Based Indoor Localization Algorithm With Backscatter Information of Passive UHF RFID Tags. *IEEE Sens. J.* **2017**, *17*, 185–193. [[CrossRef](#)]
26. Iannello, F.; Simeone, O.; Spagnolini, U. Energy Management Policies for Passive RFID Sensors with RF-Energy Harvesting. In Proceedings of the 2010 IEEE International Conference on Communications, Cape Town, South Africa, 23–27 May 2010; pp. 1–6. [[CrossRef](#)]
27. Adami, S.E.; Proynov, P.; Hilton, G.S.; Yang, G.; Zhang, C.; Zhu, D.; Li, Y.; Beeby, S.P.; Craddock, I.J.; Stark, B.H. A Flexible 2.45-GHz Power Harvesting Wristband with Net System Output From -24.3 dBm of RF Power. *IEEE Trans. Microw. Theory Tech.* **2018**, *66*, 380–395. [[CrossRef](#)]
28. Lee, W.J.; Shah, S.T.; Munir, D.; Lee, T.J.; Chung, M.Y. A Mechanism on Energy Harvesting and Data Communications in Wi-Fi Network. In Proceedings of the IMCOM ’16: 10th International Conference on Ubiquitous Information Management and Communication, New York, NY, USA, 4–6 January 2016. [[CrossRef](#)]
29. Song, Z.; Sastry, C.R. Passive RF Energy Harvesting Scheme for Wireless Sensor. U.S. Patent US8552597B2, 18 September 2013.
30. Xie, K.; Liu, Y.M.; Zhang, H.L.; Fu, L.Z. Harvest the Ambient AM Broadcast Radio Energy for Wireless Sensors. *J. Electromagn. Waves Appl.* **2011**, *25*, 2054–2065. [[CrossRef](#)]
31. Vyas, R.J.; Cook, B.B.; Kawahara, Y.; Tentzeris, M.M. E-WEHP: A Batteryless Embedded Sensor-Platform Wirelessly Powered From Ambient Digital-TV Signals. *IEEE Trans. Microw. Theory Tech.* **2013**, *61*, 2491–2505. [[CrossRef](#)]
32. Piñuela, M.; Mitcheson, P.D.; Lucyszyn, S. Ambient RF Energy Harvesting in Urban and Semi-Urban Environments. *IEEE Trans. Microw. Theory Tech.* **2013**, *61*, 2715–2726. [[CrossRef](#)]
33. Omeke, K.G.; Mollel, M.; Shah, S.T.; Zhang, L.; Abbasi, Q.H.; Imran, M.A. Towards a Sustainable Internet-of-Underwater-Things based on AUVs, SWIPT and Reinforcement Learning. *IEEE Internet Things J.* **2023**, *1*. [[CrossRef](#)]
34. Kim, S.; Vyas, R.; Bitto, J.; Niotaki, K.; Collado, A.; Georgiadis, A.; Tentzeris, M.M. Ambient RF Energy-Harvesting Technologies for Self-Sustainable Standalone Wireless Sensor Platforms. *Proc. IEEE* **2014**, *102*, 1649–1666. [[CrossRef](#)]
35. Andrenko, A.S.; Lin, X.; Zeng, M. Outdoor RF Spectral Survey: A Roadmap for Ambient RF Energy Harvesting. In Proceedings of the TENCON 2015—2015 IEEE Region 10 Conference, Macao, China, 1–4 November 2015; pp. 1–4. [[CrossRef](#)]
36. Matiko, J.W.; Grabham, N.J.; Beeby, S.P.; Tudor, M.J. Review of the Application of Energy Harvesting in Buildings. *Meas. Sci. Technol.* **2013**, *25*, 012002. [[CrossRef](#)]
37. Mimis, K.; Gibbins, D.; Dumanli, S.; Watkins, G.T. Ambient RF Energy Harvesting Trial in Domestic Settings. *IET Microwaves Antennas Propag.* **2015**, *9*, 454–462. [[CrossRef](#)]
38. Sherazi, H.H.R.; Zorbas, D.; O’Flynn, B. A Comprehensive Survey on RF Energy Harvesting: Applications and Performance Determinants. *Sensors* **2022**, *22*, 2990. [[CrossRef](#)]
39. Guler, U.; Ghovanloo, M. Power Management in Wireless Power-Sipping Devices: A Survey. *IEEE Circuits Syst. Mag.* **2017**, *17*, 64–82. [[CrossRef](#)]

40. Song, C.; Huang, Y.; Carter, P.; Zhou, J.; Yuan, S.; Xu, Q.; Kod, M. A Novel Six-Band Dual CP Rectenna Using Improved Impedance Matching Technique for Ambient RF Energy Harvesting. *IEEE Trans. Antennas Propag.* **2016**, *64*, 3160–3171. [[CrossRef](#)]
41. Chen, L.; Milligan, B.; Qu, T.; Jeevananthan, L.; Shaker, G.; Safavi-Naeini, S. Cellular Wireless Energy Harvesting for Smart Contact Lens Applications [Education Corner]. *IEEE Antennas Propag. Mag.* **2018**, *60*, 108–124. [[CrossRef](#)]
42. Bitto, J.; Hester, J.G.; Tentzeris, M.M. Ambient RF Energy Harvesting From a Two-Way Talk Radio for Flexible Wearable Wireless Sensor Devices Utilizing Inkjet Printing Technologies. *IEEE Trans. Microw. Theory Tech.* **2015**, *63*, 4533–4543. [[CrossRef](#)]
43. Palazzi, V.; Hester, J.; Bitto, J.; Alimenti, F.; Kallialakis, C.; Collado, A.; Mezzanotte, P.; Georgiadis, A.; Roselli, L.; Tentzeris, M.M. A Novel Ultra-Lightweight Multiband Rectenna on Paper for RF Energy Harvesting in the Next Generation LTE Bands. *IEEE Trans. Microw. Theory Tech.* **2018**, *66*, 366–379. [[CrossRef](#)]
44. Vu, H.S.; Nguyen, N.; Ha-Van, N.; Seo, C.; Thuy Le, M. Multiband Ambient RF Energy Harvesting for Autonomous IoT Devices. *IEEE Microw. Wirel. Components Lett.* **2020**, *30*, 1189–1192. [[CrossRef](#)]
45. Wagih, M.; Nesbitt, R.; Ansari, S.; Abbasi, Q.H.; Ali Imran, M. RFID-Enabled Energy Harvesting using Unidirectional Electrically-Small Rectenna Arrays. In Proceedings of the 2023 17th European Conference on Antennas and Propagation (EuCAP), Florence, Italy, 26–31 March 2023; pp. 1–4. [[CrossRef](#)]
46. Alvarez-Narciandi, G.; Laviada, J.; Pino, M.R.; Las-Heras, F. Phase Acquisition Techniques for RFID Multistatic Setups. *Sensors Actuators A Phys.* **2018**, *270*, 97–107. [[CrossRef](#)]
47. Pandey, A.; Jain, A. Comparative Analysis of KNN Algorithm Using Various Normalization Techniques. *Int. J. Comput. Netw. Inf. Secur.* **2017**, *9*, 36–42. [[CrossRef](#)]
48. Breiman, L. Random Forests. *Mach. Learn.* **2001**, *45*, 5–32. [[CrossRef](#)]

Disclaimer/Publisher’s Note: The statements, opinions and data contained in all publications are solely those of the individual author(s) and contributor(s) and not of MDPI and/or the editor(s). MDPI and/or the editor(s) disclaim responsibility for any injury to people or property resulting from any ideas, methods, instructions or products referred to in the content.